

Quantum-interference origin and magnitude of $1/f$ noise in Dirac nodal line IrO_2 nanowires at low temperatures

Po-Yu Chien,¹ Chih-Yuan Wu,² Ruey-Tay Wang,¹ Shao-Pin Chiu,¹ Stefan Kirchner,^{1,3} Sheng-Shiuan Yeh,^{3,4, a)} and Juhn-Jong Lin^{1, a)}

¹⁾Department of Electrophysics, National Yang Ming Chiao Tung University, Hsinchu 30010, Taiwan

²⁾Department of Physics, Fu Jen Catholic University, Taipei 24205, Taiwan

³⁾Center for Emergent Functional Matter Science, National Yang Ming Chiao Tung University, Hsinchu 30010, Taiwan

⁴⁾International College of Semiconductor Technology, National Yang Ming Chiao Tung University, Hsinchu 30010, Taiwan

(Dated: 20 February 2023)

We present $1/f$ noise measurements of IrO_2 nanowires from 1.7 to 350 K. Results reveal that the noise magnitude (represented by Hooge parameter γ) increases at low temperatures, indicating low-frequency resistance noise from universal conductance fluctuations. The cause of this noise is determined to be due to oxygen vacancies in the rutile structure of IrO_2 . Additionally, the number density of these mobile defects can be calculated from the \sqrt{T} resistance rise caused by the orbital two-channel Kondo effect in the Dirac nodal line metal IrO_2 .

The metal iridium dioxide (IrO_2) has drawn significant attention as a promising material for spintronic applications due to its giant spin Hall resistivity.¹ IrO_2 is also widely used in glucose and pH sensors.² Recently, the elusive orbital two-channel Kondo (2CK) effect was observed in IrO_2 nanowires (NWs).³ It results in a square-root-in-temperature increase of the resistivity, *i.e.*, $\rho \propto -\sqrt{T}$ (where ρ is resistivity, and T is temperature) below a characteristic temperature due to oxygen vacancies (V_O 's).³ These observations make IrO_2 NWs an attractive platform for exploring strongly correlated electron systems.⁴ Despite its potential, there is limited information on the low- T low-frequency $1/f$ noise and its origin in IrO_2 . The $1/f$ noise is a key factor which will ultimately limit the performance of every nanoelectronic device.⁵

The standard theory of $1/f$ noise in metals assumes the existence of mobile defects, often modeled as a set of independent two-level systems (TLSs) with a wide distribution of relaxation times. It can be shown that the resulting resistance fluctuations power spectrum density (PSD) possesses a $1/f^\alpha$ dependence, with $\alpha \simeq 1$.⁶⁻⁸ In this study, we examine the relationship between the number density of mobile defects (n_m) in IrO_2 NWs and the $1/f$ noise measured within the T range of 1.7 to 350 K. We find unexpected results at low T , where the noise magnitude increases with decreasing T . We explain that this low- T $1/f$ noise originates from the universal conductance fluctuations (UCF), which stem from quantum interference of conduction electrons scattered off mobile defects.⁹⁻¹¹ We identify these mobile defects are associate with the V_O 's in the IrO_2 rutile structure. While $1/f$ noise has been measured in a wide variety of conductors, both the origin and the amount of the underlying mobile defects in a given material are usually difficult to identify and quantize. In the present case, we demonstrate that combined with the measurements of the 2CK effect, the n_m value in every NW can be inferred.

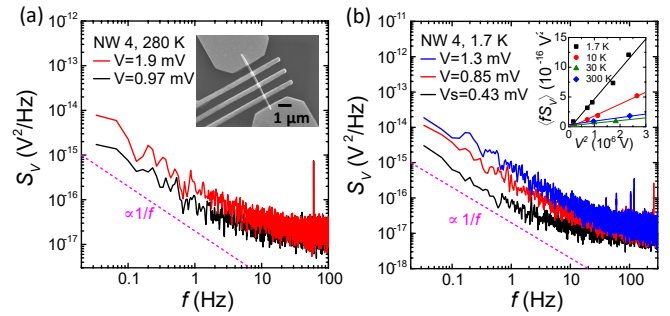


FIG. 1. Voltage power spectrum density as a function of frequency for NW 4 at (a) 280 K and (b) 1.7 K. The dashed line is drawn proportional to $1/f$ and is a guide to the eye. Insets: (a) an SEM image of a typical IrO_2 NW device, and (b) $\langle fS_V \rangle$ versus V^2 at four T values.

Our IrO_2 NWs were grown via the metal-organic chemical vapor deposition method.^{12,13} The single-crystalline rutile structure was characterized by selected-area electron diffraction patterns¹² and X-ray diffraction (XRD) patterns.¹⁴ To generate V_O 's, the NWs were thermally annealed at 300°C in vacuum. The annealing time was 3 h for NWs 1 to 3, and 4 h for NW 4. To facilitate electrical measurements, submicron Cr/Au (10/120 nm) electrodes attaching a NW device were fabricated by the electron-beam lithographic technique. The inset of Fig. 1 shows a scanning electron microscopy (SEM) image of a typical NW device. An ac method for $1/f$ noise measurement was applied.¹⁵ The background voltage noise PSD in our setup was $S_V^0 \approx 1.6 \times 10^{-17}$ V²/Hz, which was limited by the voltage preamplifier (Stanford Research model SR560). The relevant parameters of the four IrO_2 NWs studied in the present work are listed in Table I.

Power spectrum density and Hooge parameter γ . For an ohmic conductor under a small bias current I , the measured voltage noise is usually expressed by the empirical form¹⁶

$$S_V = \frac{\gamma}{N_c f^\alpha} V^2 + S_V^0, \quad (1)$$

^{a)} Authors to whom correspondence should be addressed: ssyeh@nycu.edu.tw (S.S.Y.) and jjlin@nycu.edu.tw (J.J.L.)

TABLE I. Relevant parameters for IrO₂ NWs. L is the NW length between the voltage probes in a 4-probe configuration, d is the NW diameter, $n_m^{2\text{CK}}$ is number density of mobile defects determined from the 2CK effect, n_i is number density of total (static and mobile) defects, L_e is electron elastic mean free path, and L_ϕ is electron dephasing length. $(L_e/L_\phi)^2$ is calculated with $L_\phi \simeq 100$ nm.

Nanowire	L (μm)	d (nm)	$n_m^{2\text{CK}}$ (m^{-3})	$n_m^{2\text{CK}}/n_i$	$(L_e/L_\phi)^2$
NW 1	1.9	143	7.5×10^{25}	0.074	0.0015
NW 2	1.0	123	1.8×10^{25}	0.020	0.0019
NW 3	0.75	125	3.4×10^{25}	0.037	0.0018
NW 4	0.90	147	7.8×10^{25}	0.065	0.0010

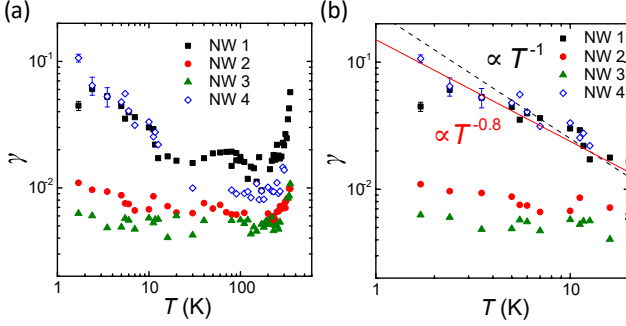


FIG. 2. (a) Hooe parameter γ as a function of temperature for four IrO₂ NWs between 1.7 and 350 K. Note that in NWs 1 and 4, $\gamma(2\text{K}) > \gamma(300\text{K})$. (b) γ versus T below 20 K. The straight solid line is a linear fit to NW 4. The straight dashed line is a guide to the eye. In NW 1, γ saturates below about 3 K.

where γ is the Hooe parameter which characterizes the $1/f$ noise magnitude, N_c is the total carrier number in the sample, V is the voltage dropped on the sample.

Figures 1(a) and (b) show the measured S_V of NW 4 at two representative temperatures 280 and 1.7 K, respectively. Above several tens Hz, the measured S_V approaches a constant ($\approx S_V^0$). At lower frequencies, S_V increases with decreasing f , as well as with increasing V . A $S_V \propto f^{-\alpha}$ dependence, with $\alpha \simeq 1$, is found for $f \lesssim 1$ Hz. This dependence can be well described by Eq. (1). To extract the γ value, we rewrite Eq. (1) as $\langle fS_V \rangle = \langle \gamma V^2/N_c \rangle + \langle fS_V^0 \rangle = \gamma V^2/N_c + \langle f \rangle S_V^0$, where $\langle fS_V \rangle$ denotes the average of the product of each discrete f_i and S_{V_i} in the data set in the $S_V \propto 1/f$ regime. The inset of Fig. 1(b) shows that our data obey the $\langle fS_V \rangle \propto V^2$ dependence at our measurement temperatures. Thus, the γ value can be obtained from a linear fit of the slope γ/N_c , where $N_c = n_c L d^2$, with $n_c \approx 1 \times 10^{28} \text{ m}^{-3}$ being the carrier density of IrO₂,¹⁷ L (d) the length (diameter) of the NW. The linear dependence $\langle fS_V \rangle \propto V^2$ suggests that the measured voltage noise originates from the resistance fluctuations in the NW, *i.e.*, the (small) applied I only acts as a sensitive electrical probe, while it does not drive the resistance fluctuations.¹⁶

The extracted γ values as a function of T between 1.7 and 350 K for four IrO₂ NWs are plotted in Fig. 2(a). As T decreases from 350 K, γ first decreases and then saturates below around 100 K. For example, the γ value of NW 4 decreases

from ≈ 0.014 at 300 K to ≈ 0.009 at 100 K, and then remains constant until about 20 K. In this high- T regime, we expect that the TLSs are thermally activated and the $1/f$ noise essentially follows the local-interference model.¹⁸ In the rest of this Letter, we shall focus our discussion on the noise below 20 K, which results from the UCF in the NWs.

UCF-induced $1/f$ noise. The most interesting observation of this work is that, below about 20 K, our extracted γ values increase with decreasing T in all NWs. This extraordinary behavior is particularly significant in NWs 1 and 4. In NW 4, the value of γ at 1.7 K is $\simeq 0.11$ [$\gamma(1.7\text{K}) \simeq 0.11$] and is one order of magnitude larger than that at 30 K, and even larger than that at 300 K. Figure 2(b) shows that NW 1 has $\gamma(T)$ behavior similar to that of NW 4, except that the γ value saturates below ~ 3 K. The low- T increase of γ in NWs 2 and 3 is smaller than that in NWs 1 and 4.

The rapid and repeated switching of mobile defects or TLSs modifies (a large fraction of) the electron paths traversing the NW. The resulting quantum interference among the electron trajectories is sensitively altered. The interference effect becomes more pronounced at lower T , where the electron dephasing time (τ_ϕ) well surpasses the electron elastic mean free time (τ_e), *i.e.*, $\tau_\phi \gg \tau_e$. This is the origin of the temporal UCF.^{9,10} In 1991, Feng realized that UCF in turn could give rise to $1/f$ noise. He showed that the phenomenological Hooe parameter γ was directly connected with the variance of the conductance fluctuations, and given by,^{9,10}

$$\gamma = \frac{N_c}{\ln(f_{\text{max}}/f_{\text{min}})} \frac{\delta G^2}{G^2}, \quad (2)$$

where f_{max} (f_{min}) denotes the maximum (minimum) frequency of the mobile defects which are relevant in the measurement, G is the conductance of the sample, and δG^2 is the variance of the UCF. Because $\delta G^2/G^2$ increases as the quantum-interference effect increases, γ grows with decreasing T . An additional T -dependence of $\delta G^2/G^2$ may be due to the saturation of τ_ϕ (*i.e.*, τ_ϕ becomes nearly independent of T) as $T \rightarrow 0$.¹⁹

As the electron dephasing length $L_\phi = \sqrt{D\tau_\phi} < L, d$, where $D = v_F^2 \tau_e/3$ is the electron diffusion constant and v_F is the Fermi velocity, our NWs are essentially three-dimensional (3D). We consider the UCF in the ‘‘saturated’’ regime, which is defined by $n_m/n_i \gg (L_e/L_\phi)^2$, where $n_i = 1/L_e \langle \sigma \rangle$ is the number density of total (static and mobile) defects, $L_e = v_F \tau_e$ is the electron elastic mean free path, and $\langle \sigma \rangle$ is the averaged electron scattering cross section. This is the regime that is pertinent to our NWs, see Table I. The UCF theory predicts under these conditions the normalized variance¹⁰

$$\frac{\delta G^2}{G^2} = 28.2 \frac{1}{k_F^4 L_e^2 L d^2}, \quad (3)$$

where k_F is the Fermi wavenumber. Thus, the T dependence is fully determined by the T behavior of L_ϕ . In writing down Eq. (3), the thermal energy averaging effect has been ignored which presumably would introduce another characteristic length scale, the thermal diffusion length $L_T = \sqrt{D\hbar/k_B T}$, into the cutoff of the UCF (\hbar is the Planck constant divided

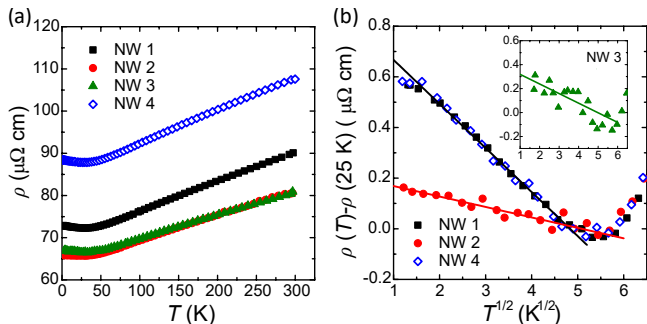


FIG. 3. (a) Resistivity versus temperature for four IrO₂ NWs. The data reveal typical metallic behavior above ~ 25 K. At lower T , ρ increases with decreasing T . (b) Main panel and inset: $[\rho(T) - \rho(25 \text{ K})]$ versus \sqrt{T} . The straight lines are linear fits to Eq. (4).

by 2π , and k_B is the Boltzmann constant). We have previously found that the thermal energy averaging effect on the UCF magnitude was negligibly smaller than theoretically predicted.²⁰ Thus, we take Eq. (3) to be sufficient for providing a good understanding of the $\gamma(T)$ data.

Figure 2(b) shows that below about 20 K, $\gamma \propto L_\varphi \propto T^{-0.8}$ in NW 4. This T dependence can be readily explained in terms of an electron dephasing rate $1/\tau_\varphi(T) = 1/\tau_\varphi^0 + 1/\tau_{e-ph}(T)$, where the first term $1/\tau_\varphi^0$ has been widely observed in experiments and is called the saturated electron dephasing rate as $T \rightarrow 0$.¹⁹ The second term $1/\tau_{e-ph} \propto T^2$ is the electron-phonon scattering rate which dominates the inelastic scattering in weakly disordered metals.^{21,22} In NW 1, γ shows a similar T behavior until it saturates below about 3 K, indicating that $1/\tau_\varphi^0$ is much larger in this NW than in NW 4.²³ The magnitudes of γ increase in NWs 2 and 3 are small, because these two NWs have comparatively small n_m values (see below).

Identifying the origin and number density of mobile defects. We will now delve into the examination of the microscopic source of mobile defects responsible for inducing UCF and determining the $1/f$ noise magnitude in IrO₂ NWs, including their number density. This is based on nonmagnetic orbital 2CK physics which was recently reported in this material. The 2CK effect in IrO₂ causes a \sqrt{T} increase of ρ at low T . Figure 3(a) shows the variation of ρ with T for our NWs. $\rho(T)$ reveals typical Boltzmann transport behavior until below about 25 K where it slightly increases with decreasing T . Close inspection indicates that this increase obeys a \sqrt{T} dependence down to 2 K, Fig. 3(b). Between 2 and 25 K, the normalized increase is $[\rho(2 \text{ K}) - \rho(25 \text{ K})]/\rho(25 \text{ K}) \approx (2.2 - 7.7) \times 10^{-3}$ in our NWs. This amount of resistivity increase is more than one order of magnitude larger than what would be expected from the 3D weak localization and electron-electron interaction effects.^{3,24} We have recently demonstrated that this \sqrt{T} increase obeys²⁵

$$\rho_{2\text{CK}}(T) = \frac{3n_m^{2\text{CK}}}{4\pi\hbar[eN(0)v_F]^2} \left(1 - 4\sqrt{\frac{\pi T}{T_{2\text{CK}}}}\right), \quad (4)$$

where $n_m^{2\text{CK}}$ denotes the number density of 2CK scatterers, $N(0)$ is the density of states at the Fermi energy per spin per

channel, and $T_{2\text{CK}}$ is a characteristic temperature scale in the 2CK problem.

Oxygen vacancies frequently occur in IrO₂ which assumes the rutile structure, depending on the sample preparation conditions.³ Due to charge neutrality, a V_O generates two “defect electrons” in IrO₂. One of the two defect electrons, which occupies the doubly degenerate $5d_{xz}$ or $5d_{yz}$ iridium ion orbital, is strongly coupled to the two equivalent and independent spin-up and spin-down conduction-electron channels. This is the origin of the 2CK effect in IrO₂.^{3,4} With the assumption that the density of V_O ’s, denoted by n_{V_O} , is low enough to safely ignore any correlations between V_O ’s, we can estimate $n_{V_O} \simeq n_m^{2\text{CK}}$ in each IrO₂ NW.

To compare our data with Eq. (4), we take $T_{2\text{CK}} \simeq 23$ K, the temperature below which the \sqrt{T} behavior is found. Then, the $n_m^{2\text{CK}}$ value in each NW can be extracted from the fitted slope plotted in Fig. 3(b), using $N(0) \approx 1.5 \times 10^{27} \text{ J}^{-1} \text{ m}^{-3}$ and $v_F \approx 5 \times 10^5 \text{ m/s}$ for IrO₂.^{3,26} These values are listed in Table I. We see that NWs 1 and 4, which have the largest noise magnitudes γ , also show the largest \sqrt{T} resistivity increases (*i.e.*, largest $n_m^{2\text{CK}}$ values), and NWs 2 and 3 have smaller noise magnitudes and simultaneously smaller resistivity increases (*i.e.*, smaller $n_m^{2\text{CK}}$ values).

In practice, the mobile defects existing in a given sample may not all contribute to a given noise measurement, and n_m will be given by the number of those defects having switching frequency $f_{\text{min}} \leq f \leq f_{\text{max}}$. Then, $n_m \lesssim n_{V_O} \simeq n_m^{2\text{CK}}$. In the regime where the resistance fluctuations are governed by the local-interference (LI) mechanism and $n_{V_O} \approx n_m^{2\text{CK}}$ holds, we obtain an estimate for the switching TLS density n_m^{LI} . This is accomplished by applying a method developed earlier,²⁷ where n_m^{LI} can be estimated with the measured γ value through $n_m^{\text{LI}} \approx 4\pi\gamma n_e (\rho e^2 / mv_F \langle \sigma \rangle)^2$, where e (m) is the electronic charge (effective mass). At 30 K, this gives in the present case $n_m^{\text{LI}} \approx (1.9 \pm 0.1) \times 10^{25} \text{ m}^{-3}$ for NWs 1 and 4, and $\approx (5.5 \pm 1) \times 10^{24} \text{ m}^{-3}$ for NWs 2 and 3. These extracted n_m^{LI} values scale with and are smaller than the n_{V_O} values within a factor of 10, indicating the fluctuators at low T are associated with the V_O ’s. Thus, in our NWs, we estimate n_m [$\sim n_m^{\text{LI}}(30 \text{ K}) \lesssim n_{V_O} \simeq n_m^{2\text{CK}}$] has values $\sim 10^{24} - 10^{25} \text{ m}^{-3}$, being about one order of magnitude larger than that found in, *e.g.*, Bi films.²⁸

One possible explanation for this is the existence of an interstitial oxygen density that is (by and large) proportional to n_{V_O} . Our thermal annealing studies suggest that this is not the reason for the proportionality between n_{V_O} and n_m^{LI} , as an increase in annealing time in vacuum is expected to reduce the number density of oxygen interstitials while increasing n_{V_O} . This leaves us with the more interesting alternative that the V_O ’s themselves are driving the $1/f$ noise.

The characteristic feature of the one-channel (two-channel) Kondo effect is the existence of a degenerate local level hybridizing with a band (two bands) of electron states. This leads to a characteristic energy scale known as the Kondo temperature (T_K) or equivalently a characteristic time scale $\tau_K = \hbar/k_B T_K$.²⁹ (In the present case, $T_K = T_{2\text{CK}}$.) On the other hand, $1/f$ noise is associated with a broad distribution of relaxation times of the mobile defects. To ensure that the

2CK effect can form in IrO_2 , the degeneracy between $5d_{xz}$ and $5d_{yz}$ has to remain intact even in the presence of such a broad distribution. Moreover, to guarantee that the flickering is not interfering with the formation of the 2CK effect, $k_B T_{2\text{CK}} \gg hf$ needs to hold. This is evidently satisfied, as can be inferred from Fig. 1 with $T_{2\text{CK}} \approx 20$ K as is appropriate for IrO_2 NWs. The necessary broad distribution of relaxation times of the fluctuators driving the $1/f$ noise implies a corresponding disorder distribution of the V_O environment. That the T_K value distribution in such a situation remains sharply peaked has been addressed before.³⁰ A microscopic model of how V_O 's can drive an orbital Kondo effect and concomitantly $1/f$ noise at lower frequencies is left for future work. Intuitively, if different V_O 's reside at varying distances to grain boundaries, and grain boundaries in the NW have differing orientations, a distribution of the relaxation times should naturally arise. NW surfaces (and the interface with substrate) could likely have similar effects on resulting in a distribution of relaxation times. In any case, our recent experiments have confirmed that the $1/f$ noise magnitude in a series of RuO_2 films is controlled by n_{V_O} , which can be reversely adjusted, *i.e.*, increased or reduced, by annealing RuO_2 in vacuum, air, or oxygen gas.²⁷ Since both RuO_2 and IrO_2 crystallize in the rutile structure and have similar physical properties³¹ (except that RuO_2 is antiferromagnetic which leads to an orbital one-channel Kondo effect at low T , see Ref. 3), we expect that V_O 's play a similar role in producing $1/f$ noise in IrO_2 .

Temporal resistance fluctuations. While the UCF-induced $1/f$ noise has been theoretically proposed in the 1980s,³² the predictions have not been widely tested. The reasons are that one needs to use microscale samples and measure the noise down to low T . Otherwise, the quantum-interference effect will be negligible and the noise magnitude small and difficult to detect. To further check that the measured $1/f$ noise in IrO_2 below 20 K is caused by the UCF mechanism, we have extracted the (normalized) variance of conductance fluctuations $\delta G^2/G^2$ from an independent measurement, and compare it with that calculated from the measured γ value through Eq. (2).

In our experimental method, a current I is applied to the NW device and the total voltage fluctuations $\delta V_m(t)$ are measured, *i.e.*, $\delta V_m(t) = I\delta R(t) + \delta V_0(t)$, where $I\delta R$ is the voltage noise of the NW, and δV_0 is the input noise of the preamplifier. Figure 4(a) shows the measured $\delta V_m(t)$ at several I values for NW 4 at 1.7 K. We see that the δV_m magnitude increases with increasing I . The $\delta G^2/G^2$ value of a NW can be obtained by subtracting out the background contribution δV_0 . Because $\delta R(t)$ and $\delta V_0(t)$ are uncorrelated, we write $\delta V_m^2 = I^2 \delta R^2 + \delta V_0^2$ for an ohmic conductor, where δV_m^2 , δR^2 , and δV_0^2 denote the variances of $\delta V_m(t)$, $\delta R(t)$, and $\delta V_0(t)$, respectively. Thus, the intrinsic resistance fluctuations of the NW δR^2 can be obtained from a plot of δV_m^2 versus I^2 . Figure 4(b) shows the variation of δV_m^2 with I^2 for our NWs at 1.7 K. A $\delta V_m^2 \propto I^2$ linear dependence is observed for all NWs, with the fitted $\delta V_0^2 \approx (5.5 \pm 0.2) \times 10^{-15} \text{ V}^2$. Here we note that in our noise measurements, the sampling rate of the spectrum analyzer (Stanford Research model SR785) was set to be 1024 Hz and the measurement time was lasted for 30 s, cor-

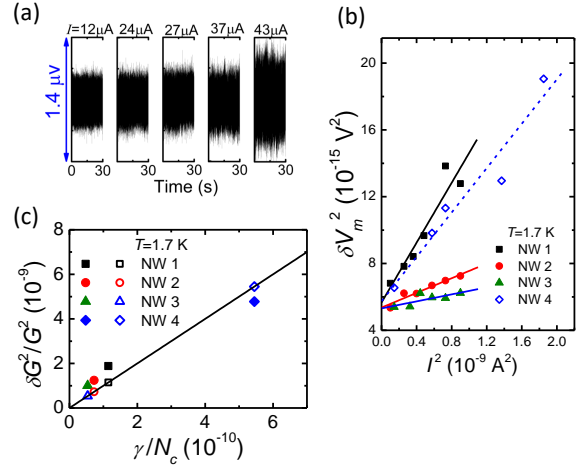


FIG. 4. (a) Voltage fluctuations as a function of time for NW 4 at 1.7 K and under five different bias currents. (b) δV_m^2 versus I^2 . Straight solid and dashed lines are linear fits. (c) $\delta G^2/G^2$ versus γ/N_c . Closed symbols are calculated from δV_m^2 . Open symbols are calculated through Eq. (2). The straight line is a guide to the eye.

responding to the relevant frequency range from $f_{\min} \simeq 0.033$ Hz to $f_{\max} \simeq 512$ Hz. This f range leads to an estimated upper bound $\delta V_0^2 \sim S_V^0 \times (f_{\max} - f_{\min}) \sim 8 \times 10^{-15} \text{ V}^2$, being in good accord with our measurement.

Once δR^2 value in each NW is obtained from the slope in Fig. 4(b), $\delta G^2/G^2 = \delta R^2/R^2$ can be calculated. The calculated $\delta G^2/G^2$ values (solid symbols) as a function of the normalized Hooge parameter γ/N_c are plotted in Fig. 4(c). Alternatively, we have calculated $\delta G^2/G^2$ values (open symbols) from the measured γ (Fig. 2) through Eq. (2), by inserting $\ln(f_{\max}/f_{\min}) \approx \ln(512/0.033) \approx 10$. Figure 4(c) shows that the $\delta G^2/G^2$ values obtained from the two independent methods agree to within a factor of ~ 2 . At $T = 1.7$ K, $\delta G^2/G^2 \approx 1.9 \times 10^{-9}$ and $\approx 4.8 \times 10^{-9}$ in NWs 1 and 4, respectively. We thus obtain $L_\phi \approx 95$ (81) nm in the former (the latter) through Eq. (3), where $k_F \approx 7 \times 10^9 \text{ m}^{-1}$.²⁶ Therefore, we have $L_\phi < d$ and $n_m/n_i \gg (L_e/L_\phi)^2$, justifying the application of Eq. (3).

The $1/f$ noise has previously been studied in a wide variety of metals^{6,7,9} and semiconductors,⁸ and recently, in 2D materials.^{5,33} UCF-induced $1/f$ noise were observed in polycrystalline Bi films,²⁸ Ag films,^{34,35} Au wires,²³ RuO_2 NWs,³⁶ C-Cu composites,³⁷ and epitaxial graphene.³⁸ In Bi and Ag films, the UCF fell in the “unsaturated” regime where $n_m/n_i \ll (L_e/L_\phi)^2$. The origins of the mobile defects were unspecified in those samples, while the diffusion of H atoms (the spin-glass freezing process) was identified as the cause in amorphous Ni-Zr films³⁹ (narrow AuFe wires⁴⁰). In the present study, we are able to show that V_O 's are rich and generate mobile defects in IrO_2 .

In summary, we have measured the $1/f$ noise of four IrO_2 nanowires in the temperature range from 1.7 to 350 K. As temperature decreases from 350 K, the γ value decreases down to about 100 K and then remains constant, but as $T \lesssim 20$ K γ increases with decreasing temperature. We explain this

low-temperature γ increase in terms of the UCF-induced $1/f$ noise. We identify the mobile defects to be associated with oxygen vacancies in the IrO_2 rutile structure. In combination with the orbital 2CK effect previously observed in this Dirac nodal line metal, we have extracted the number density of the mobile defects. The UCF origin of the $1/f$ noise is further confirmed by independent measurements of temporal conductance fluctuations in the nanowires.

ACKNOWLEDGMENTS

We thank C. W. Wu for experimental help. This work was supported by National Science and Technology Council of Taiwan through grant numbers 110-2112-M-A49-015 and 111-2119-M-007-005 (J.J.L.), and 110-2112-M-A49-033-MY3 (S.S.Y.).

REFERENCES

- ¹K. Fujiwara, Y. Fukuma, J. Matsuno, H. Idzuchi, Y. Niimi, Y. Otani, and H. Takagi, “5d iridium oxide as a material for spin-current detection,” *Nat. Commun.* **4**, 2893 (2013).
- ²Q. Dong, D. Song, Y. Huang, Z. Xu, J. H. Chapman, W. S. Willis, B. Li, and Y. Lei, “High-temperature annealing enabled iridium oxide nanofibers for both non-enzymatic glucose and solid-state pH sensing,” *Electrochim. Acta* **281**, 117 (2018).
- ³S. S. Yeh, T. K. Su, A. S. Lien, F. Zamani, J. Kroha, C. C. Liao, S. Kirchner, and J. J. Lin, “Oxygen vacancy-driven orbital multichannel kondo effect in dirac nodal line metals IrO_2 and RuO_2 ,” *Nat. Commun.* **11**, 4749 (2020).
- ⁴S. Kirchner, “Two-channel Kondo physics: From engineered structures to quantum materials realizations,” *Adv. Quantum Technol.* **3**, 1900128 (2020).
- ⁵A. A. Balandin, “Low-frequency $1/f$ noise in graphene devices,” *Nat. Nanotechnol.* **8**, 549 (2013).
- ⁶P. Dutta and P. M. Horn, “Low-frequency fluctuations in solids: $1/f$ noise,” *Rev. Mod. Phys.* **53**, 497 (1981).
- ⁷M. B. Weissman, “ $1/f$ noise and other slow, nonexponential kinetics in condensed matter,” *Rev. Mod. Phys.* **60**, 537 (1988).
- ⁸D. M. Fleetwood, “ $1/f$ noise and defects in microelectronic materials and devices,” *IEEE Trans. Nucl. Sci.* **62**, 1462 (2015).
- ⁹N. Giordano, “Conductance fluctuations and low-frequency noise in small disordered systems: experiment,” in *Mesoscopic Phenomena in Solids*, edited by B. L. Altshuler, P. A. Lee, and R. A. Webb (Elsevier, New York, 1991).
- ¹⁰S. Feng, “Conductance fluctuations and $1/f$ noise magnitudes in small disordered structures: theory,” in *Mesoscopic Phenomena in Solids*, edited by B. L. Altshuler, P. A. Lee, and R. A. Webb (Elsevier, New York, 1991).
- ¹¹M. S. Gupta, “Conductance fluctuations in mesoscopic conductors at low temperatures,” *IEEE Trans. Electron Devices* **41**, 2093 (1994).
- ¹²R. S. Chen, Y. S. Huang, Y. M. Liang, C. S. Hsieh, D. S. Tsai, and K. K. Tiong, “Field emission from vertically aligned conductive IrO_2 nanorods,” *Appl. Phys. Lett.* **84**, 1552 (2004).
- ¹³Y. H. Lin, Y. C. Sun, W. B. Jian, H. M. Chang, Y. S. Huang, and J. J. Lin, “Electrical transport studies of individual IrO_2 nanorods and their nanorod contacts,” *Nanotechnology* **19**, 045711 (2008).
- ¹⁴R. Chen, H. Chang, Y. Huang, D. Tsai, S. Chattopadhyay, and K. Chen, “Growth and characterization of vertically aligned self-assembled IrO_2 nanotubes on oxide substrates,” *J. Cryst. Growth* **271**, 105 (2004).
- ¹⁵J. H. Scofield, “ac method for measuring low-frequency resistance fluctuation spectra,” *Rev. Sci. Instrum.* **58**, 985 (1987).
- ¹⁶F. Hooge, “ $1/f$ noise is no surface effect,” *Phys. Lett. A* **29**, 139 (1969).
- ¹⁷J. K. Kawasaki, C. H. Kim, J. N. Nelson, S. Crisp, C. J. Zollner, E. Biegenwald, J. T. Heron, C. J. Fennie, D. G. Schlom, and K. M. Shen, “Engineering carrier effective masses in ultrathin quantum wells of IrO_2 ,” *Phys. Rev. Lett.* **121**, 176802 (2018).
- ¹⁸J. Pelz and J. Clarke, “Quantitative “local-interference” model for $1/f$ noise in metal films,” *Phys. Rev. B* **36**, 4479 (1987).
- ¹⁹J. J. Lin and J. P. Bird, “Recent experimental studies of electron dephasing in metal and semiconductor mesoscopic structures,” *J. Phys.: Condens. Matter* **14**, R501 (2002).
- ²⁰P. Y. Yang, L. Y. Wang, Y. W. Hsu, and J. J. Lin, “Universal conductance fluctuations in indium tin oxide nanowires,” *Phys. Rev. B* **85**, 085423 (2012).
- ²¹Y. L. Zhong, A. Sergeev, C. D. Chen, and J. J. Lin, “Direct observation of electron dephasing due to inelastic scattering from defects in weakly disordered AuPd wires,” *Phys. Rev. Lett.* **104**, 206803 (2010).
- ²²Y. L. Zhong and J. J. Lin, “Observation of a linear mean-free-path dependence of the electron-phonon scattering rate in thick AuPd films,” *Phys. Rev. Lett.* **80**, 588 (1998).
- ²³A. Trionfi, S. Lee, and D. Natelson, “Time-dependent universal conductance fluctuations in mesoscopic Au wires: Implications,” *Phys. Rev. B* **75**, 104202 (2007).
- ²⁴P. A. Lee and T. V. Ramakrishnan, “Disordered electronic systems,” *Rev. Mod. Phys.* **57**, 287 (1985).
- ²⁵I. Affleck and A. W. W. Ludwig, “Exact conformal-field-theory results on the multichannel Kondo effect: Single-fermion green’s function, self-energy, and resistivity,” *Phys. Rev. B* **48**, 7297 (1993).
- ²⁶J. J. Lin, W. Xu, Y. L. Zhong, J. H. Huang, and Y. S. Huang, “Electron-electron scattering times in low-diffusivity thick RuO_2 and IrO_2 films,” *Phys. Rev. B* **59**, 344 (1999).
- ²⁷S. S. Yeh, K. H. Gao, T. L. Wu, T. K. Su, and J. J. Lin, “Activation energy distribution of dynamical structural defects in RuO_2 films,” *Phys. Rev. Appl.* **10**, 034004 (2018).
- ²⁸N. O. Birge, B. Golding, and W. H. Haemmerle, “Electron quantum interference and $1/f$ noise in bismuth,” *Phys. Rev. Lett.* **62**, 195 (1989).
- ²⁹A. C. Hewson, *The Kondo Problem to Heavy Fermions* (Cambridge University Press, Cambridge, 1993).
- ³⁰S. Chakravarty and C. Nayak, “A Kondo impurity in a disordered metal: Anderson’s theorem revisited,” *Int. J. Mod. Phys. B* **14**, 1421 (2000).
- ³¹J. J. Lin, S. M. Huang, Y. H. Lin, T. C. Lee, H. Liu, X. X. Zhang, R. S. Chen, and Y. S. Huang, “Low temperature electrical transport properties of RuO_2 and IrO_2 single crystals,” *J. Phys. Condens. Matter* **16**, 8035 (2004).
- ³²S. Feng, P. A. Lee, and A. D. Stone, “Sensitivity of the conductance of a disordered metal to the motion of a single atom: Implications for $1/f$ noise,” *Phys. Rev. Lett.* **56**, 1960 (1986).
- ³³P. Karnatak, T. Paul, S. Islam, and A. Ghosh, “ $1/f$ noise in van der Waals materials and hybrids,” *Adv. Phys.: X* **2**, 428 (2017).
- ³⁴T. L. Meisenheimer and N. Giordano, “Conductance fluctuations in thin silver films,” *Phys. Rev. B* **39**, 9929 (1989).
- ³⁵P. McConville and N. O. Birge, “Weak localization, universal conductance fluctuations, and $1/f$ noise in Ag,” *Phys. Rev. B* **47**, 16667 (1993).
- ³⁶A. S. Lien, L. Y. Wang, C. S. Chu, and J. J. Lin, “Temporal universal conductance fluctuations in RuO_2 nanowires due to mobile defects,” *Phys. Rev. B* **84**, 155432 (2011).
- ³⁷G. A. Garfunkel, G. B. Alers, M. B. Weissman, J. M. Mochel, and D. J. VanHarlingen, “Universal-conductance-fluctuation $1/f$ noise in a metal-insulator composite,” *Phys. Rev. Lett.* **60**, 2773 (1988).
- ³⁸C. C. Kalmbach, F. J. Ahlers, J. Schurr, A. Müller, J. Feilhauer, M. Kruskopf, K. Pierz, F. Hohls, and R. J. Haug, “Nonequilibrium mesoscopic conductance fluctuations as the origin of $1/f$ noise in epitaxial graphene,” *Phys. Rev. B* **94**, 205430 (2016).
- ³⁹G. B. Alers, M. B. Weissman, R. S. Averback, and H. Shyu, “Resistance noise in amorphous Ni-Zr: Hydrogen diffusion and universal conductance fluctuations,” *Phys. Rev. B* **40**, 900–906 (1989).
- ⁴⁰G. Neuttiens, C. Strunk, C. Van Haesendonck, and Y. Bruynseraede, “Universal conductance fluctuations and low-temperature $1/f$ noise in mesoscopic AuFe spin glasses,” *Phys. Rev. B* **62**, 3905 (2000).